14th Joint Workshop on Physics of Strong Interacting Systems

2026.10.18-10.23 Nanjing, China

Predictions of nuclear charge radii with a physics-information machine learning approach

Weifeng Li（李伟峰）

Supervisor: Zhongming Niu（牛中明）



Contents

1 Introduction

2 Theoretical framework

3 Results and discussion

4 Summary and perspectives

01

Introduction

Introduction

安徽大学物理学院
School of Physics Anhui University

Nuclear charge radius is one of the most fundamental properties for characterizing nuclear structure.

- **Shape coexistence**

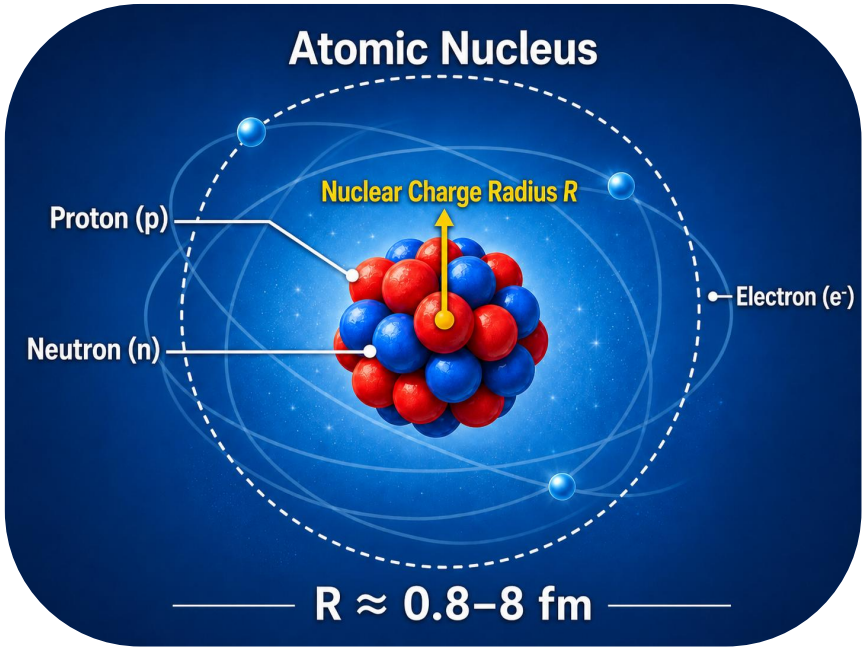
K. Heyde *et al*., RMP **83**, 1467 (2011).
X. F. Yang *et al*., PRL **116**, 182502 (2016).

- **Neutron skins**

B. A. Brown, PRL **119**, 122502 (2017).
S. J. Novario *et al*., PRL **130**, 032501 (2023).
M. Q. Ding *et al*., NST **35**, 211 (2024).
L. Wang *et al*., PRC **109**, 064303 (2024).

- **Shell structures**

T. Otsuka *et al*., RMP **92**, 015002 (2020).



- **Halo structures**

W. Geithner *et al*., PRL **101**, 252502 (2008).
W. Nörtershäuser *et al*., PRL **102**, 062503 (2009).

- **Odd-even staggering**

R. F. Garcia Ruiz *et al*., NP **12**, 594 (2016).
A. J. Miller *et al*., NP **15**, 432 (2019).
R. P. de Groote *et al*., NP **16**, 620 (2020).

- **Saturation of nuclear matter**

A. Ekström *et al*., PRC **97**, 024332 (2018).

Experimental techniques:

High-energy elastic **electron scattering**, μ-atom-excited X-ray **spectroscopy**, **Optical isotope shift** measurements, ...

Introduction

1) Empirical formula

① W. D. Myers *et al*., Nucl. Phys. A **410**, 61 (1983).
② S. Q. Zhang *et al*., Eur. Phys. J. A **13**, 285 (2002).
③ N. Wang *et al.*, Phys. Rev. C **88**, 011301(R) (2013).
④ Z. Q. Sheng *et al*, Eur. Phys. J. A **51**, 40 (2015).

2) Local-relation-based approaches

(i) Mirror-nucleus relations

① P. Bano *et al*., Phys. Rev. C **108**, 015802 (2023).
② X. Liu *et al*., Phys. Lett. B **872**, 140046 (2026).

(ii) Garvey-Kelson relations

① J. Piekarewicz *et al*., Eur. Phys. J. A **46**, 379 (2010).

3) Skyrme-Hartree-Fock-Bogoliubov (HFB)

① M. V. Stoitsov *et al*., Phys. Rev. C **68**, 054312 (2003).
② S. Goriely *et al*., Phys. Rev. Lett. **102**, 242501 (2009).
③ S. Goriely *et al*., Phys. Rev. C **82**, 035804 (2010).
④ S. Goriely *et al*., Phys. Rev. C **93**, 034337 (2016).

4) Relativistic mean-field (RMF)

① G. A. Lalazissis *et al*., At. Data Nucl. Data Tables **71**, 1 (1999).
② L. S. Geng *et al*., Prog. Theor. Phys. **110**, 921 (2003).
③ P. W. Zhao *et al*., Phys. Rev. C **82**, 054319 (2010).

5) Relativistic Hartree-Bogoliubov (RHB)

① S. E. Agbemava *et al*., Phys. Rev. C **89**, 054320 (2014).
② X. W. Xia *et al*., At. Data Nucl. Data Tables. **121-122**, 1 (2018).

6) Deformed RHB theory in continuum (DRHBc)

① K. Zhang *et al*., At. Data Nucl. Data Tables **144**, 101488 (2022).
② P. Guo *et al*., At. Data Nucl. Data Tables **158**, 101661 (2024).

7) *ab initio*

① B. R. Barrett *et al*., Prog. Part. Nucl. Phys. **69**, 131 (2013).
② A. Ekström *et al*., Phys. Rev. C **91**, 051301(R) (2015).
③ B. N. Lu *et al*., Phys. Rev. Lett. **125**, 192502 (2020).

Introduction

Machine learning in nuclear decays and reactions

▲α-decay half-lives Saxena2021JPG, Ma2021CPC

▲β-decay half-lives Niu2019PRC, Li2024JPG

▲Fission yields Wang2019PRL, Qiao2021PRC

▲Cross-sections in proton induced spallation reactions Ma2020CPC

▲Neutron-nucleus scattering data Liang2021Thesis

▲Fusion reaction cross-sections Akkoyun2020NIMB

▲……

Machine learning in nuclear structure

▲Masses Niu2018PLB, Niu2022PRC, Wu2022PLB

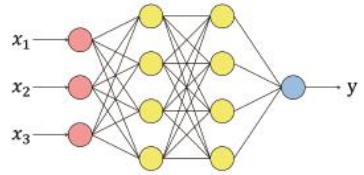
▲Nuclear spins and parities Gernoth1993PLB, Clark2006IJMPB

▲charge radii Wu2020PRC, Ma2020PRC, Dong2023PLB

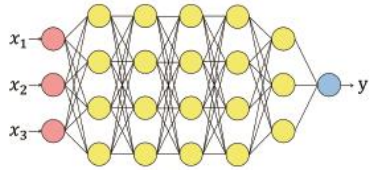
▲excited states Lasseri2020PRL, Wang2021PRC, Lv2024PLB

▲……

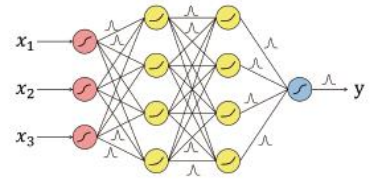
▲ANN



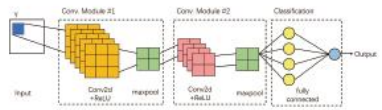
▲DNN



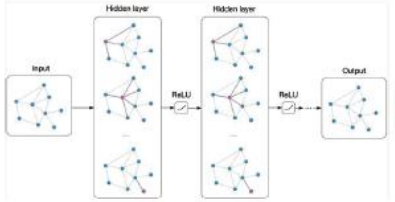
▲BNN



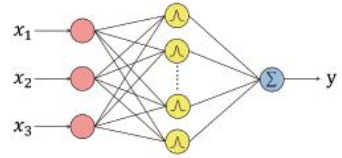
▲CNN



▲GNN



▲RBF



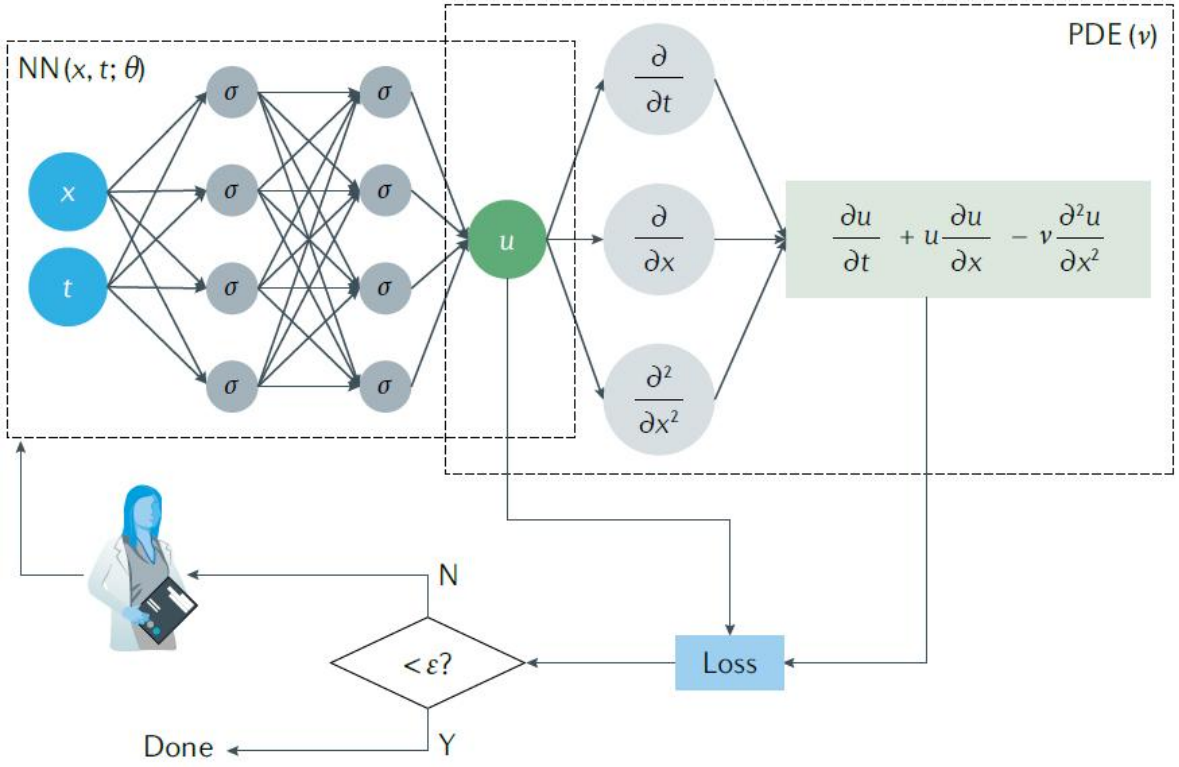
▲……

The Figure are taken from He2023SCPMA.

Introduction

安徽大学物理学院
School of Physics Anhui University

Physics Information Machine learning (PIML)



M. Raissi *et al*., J. Comput. Phys. **378**, 686 (2019).
G. E. Karniadakis *et al*., Nat. Rev. Phys. **3**, 422 (2021).

Physics information methods in nuclear physics

- Masses/Binding energies
  - Y. M. Huang *et al*., Phys. Rev. C **111**, 034329 (2025).
  - W. F. Li *et al*., Phys. Lett. B **879**, 140696 (2026).
- Charge radii
  - Z. X. Yang *et al*., Phys. Rev. C **108**, 034315 (2023).
  - T. S. Shang *et al*., Phys. Rev. C **110**, 014308 (2024).
  - Y. D. Wang *et al*., Nucl. Tech. Tech. **37**, 93 (2026).
- Reaction cross sections
  - Z. Gao *et al*., Phys. Rev. C **109**, 024601 (2024).
  - C. B. Vauterin *et al*., Nucl. Instrum Meth. B **566**, 165771 (2025).
  - H. B. Li *et al*., Chin. Phys. C **50**, 064102 (2026).
- β-decay half-lives
  - F. Minato et al., Phys. Rev. C **106**, 024306 (2022).
  - W. F. Li *et al*., Phys. Rev. C **113**, 064310 (2026).
- .....

02

Theoretical framework

Theoretical framework

安徽大学物理学院
School of Physics Anhui University

A nuclear charge radius empirical formula from Ref. [1]

$$R_{\mathrm{ch}} = \sqrt{\frac{3}{5}}\boldsymbol{r_0}\left(1-\boldsymbol{a}\frac{N-Z}{A}+\boldsymbol{b}\frac{1}{A}+\boldsymbol{c}\frac{P}{A}+\boldsymbol{d}\frac{\delta}{A}\right)A^{1/3}$$

$r_0 = 1.2297$ fm;

$a = 0.1583$;

$b = 1.9556$;

$c = 0.3623$;

$d = 0.0996$;

RMSE: 0.0289 fm

Z: Proton number;

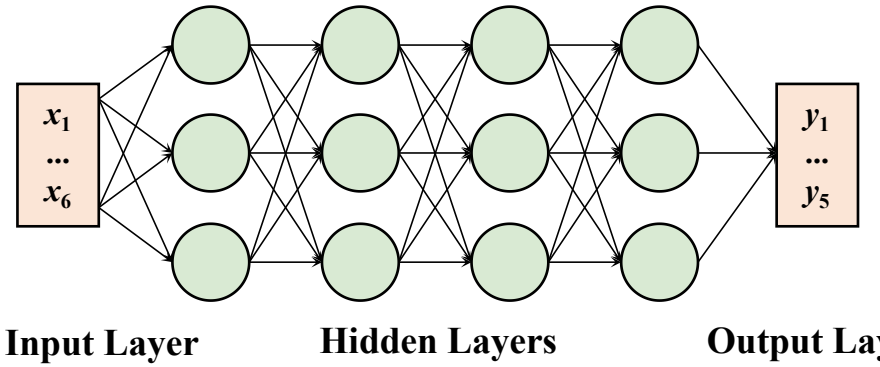
N: Neutron number;

A: Mass number;

P: $\nu_p \nu_n / (\nu_p+\nu_n)$;

δ: $[(-1)^Z + (-1)^N] / 2$

6 - 16 - 64 - 64 - 32 - 5 (r_0, *a*, *b*, *c*, *d*)



$(Z, N, A, I, \delta, P) \rightarrow (r_0, a, b, c, d)$

$$L = \frac{1}{n}\sum_{i=1}^{n}\left[R_{\mathrm{ch},i}^{\mathrm{Exp}} - \sqrt{\frac{3}{5}}\boldsymbol{r}_{0,i}^{\mathrm{NN}}\left(1-\boldsymbol{a}_i^{\mathrm{NN}}\frac{N_i-Z_i}{A_i}+\frac{\boldsymbol{b}_i^{\mathrm{NN}}}{A_i}+\boldsymbol{c}_i^{\mathrm{NN}}\frac{P_i}{A_i}+\boldsymbol{d}_i^{\mathrm{NN}}\frac{\delta_i}{A_i}\right)A_i^{1/3}\right]^2$$

[1] Z. Q. Sheng *et al.*, Eur. Phys. J. A **51**, 40 (2015).

Theoretical framework

Table I Hyperparameters of the PIML. The Dynamic Tanh (DyT) method of Ref. [1] is used as the normalization transformation.

*i*th layer	Layer	Number of neurons	Normalization	Activation function
0	Input layer	6	—	—
1	Hidden layer	16	DyT	—
2	Hidden layer	64	DyT	—
3	Hidden layer	64	DyT	Softplus
4	Hidden layer	32	DyT	Softplus
5	Output layer	5	—	—
Optimizer		Adam		
Batch size		64		
Train Epoch		10,000		
Learning rate		10^{-5} (decreased by 10^{-6} every 1,000 epoch)		

★**Learn set**： 80% nuclear charge radius in CR2013 [2] + CR2021 [3] (**811** nuclei)

★**Validation set**： 20% Nuclear charge radius in CR2013 [2] + CR2021 [3] (**203** nuclei)

★**Test set**： Nuclear charge radius that first appeared in Ref. [4] (**48** nuclei)

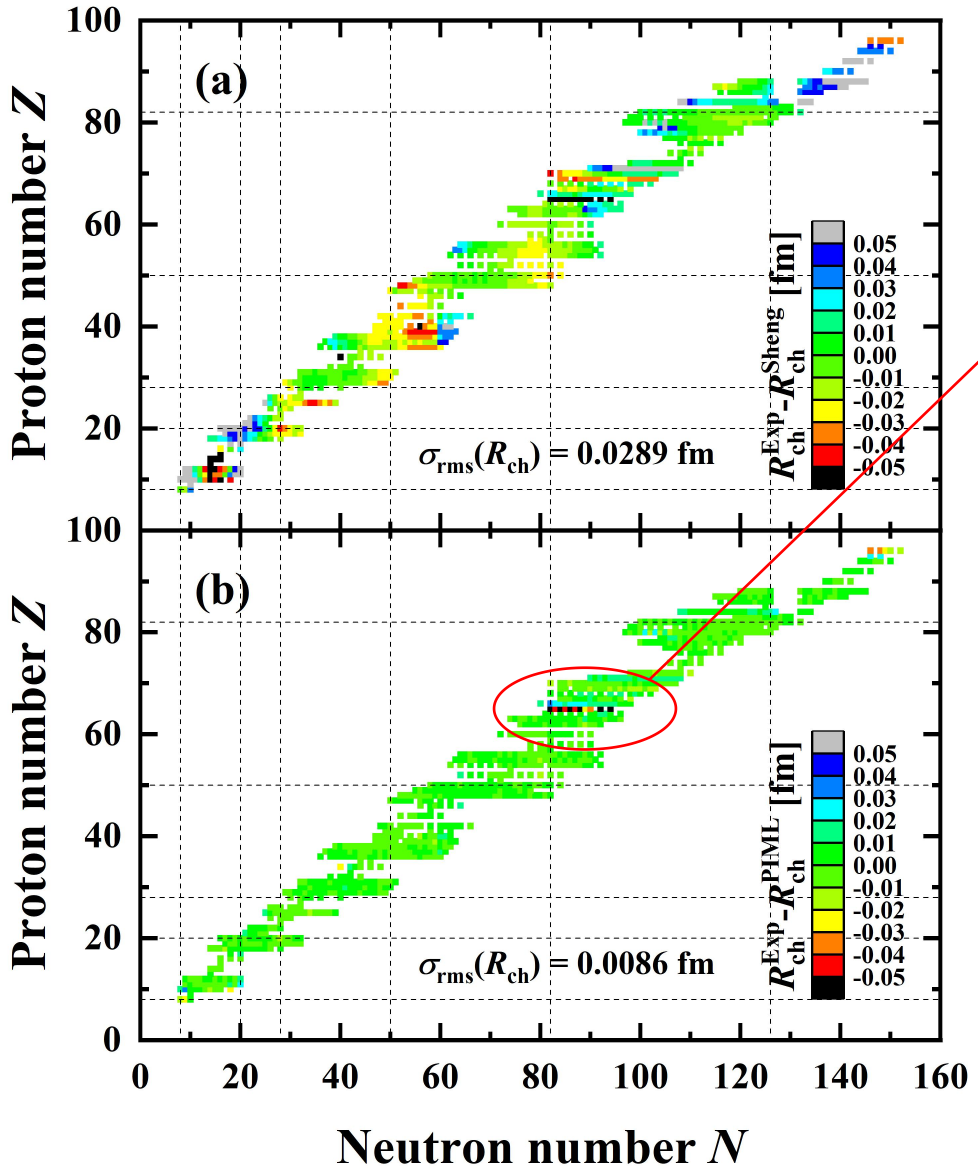
[1] J. Zhu *et al.*, Proceedings of the IEEE/CVF Conference on Computer Vision and Pattern Recognition, 14901 (2025).
[2] I. Angeli *et al.*, At. Data Nucl. Data Tables **99**, 69 (2013).
[3] T. Li *et al.*, At. Data Nucl. Data Tables **140**, 101440 (2021).
[4] C. X. Yuan *et al.*, Eur. Phys. J. A **62**, 111 (2026).

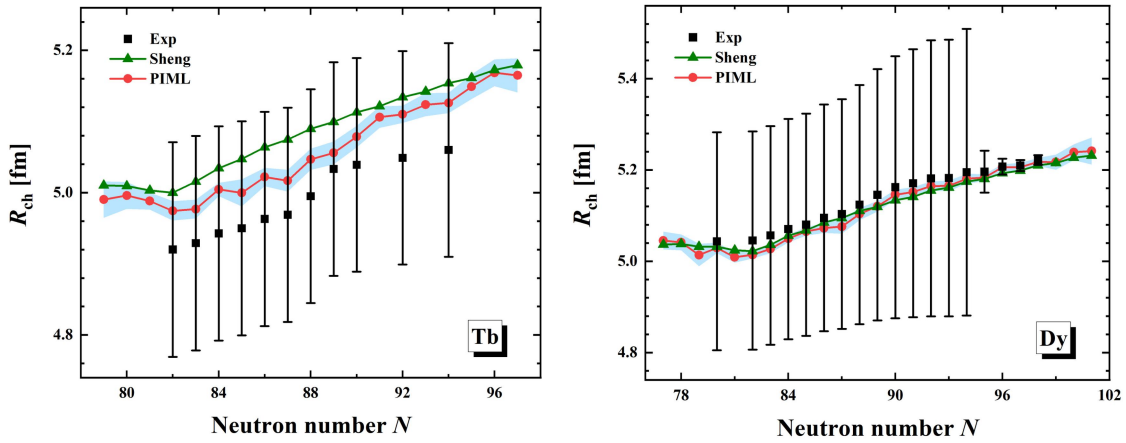
03

Results and discussion

Results and discussion

安徽大学物理学院
School of Physics Anhui University





- PIML remarkably improves the description of charge radius, even though it adopted the same function form as the Formula Sheng.
- Two approaches systematically overestimate the charge radii of the Tb isotopes.

Fig. 1 Differences between the experimental charge radii and the theoretical results with Formula Sheng and PIML. The dashed lines denote the traditional magic numbers.

Results and discussion

安徽大学物理学院
School of Physics Anhui University

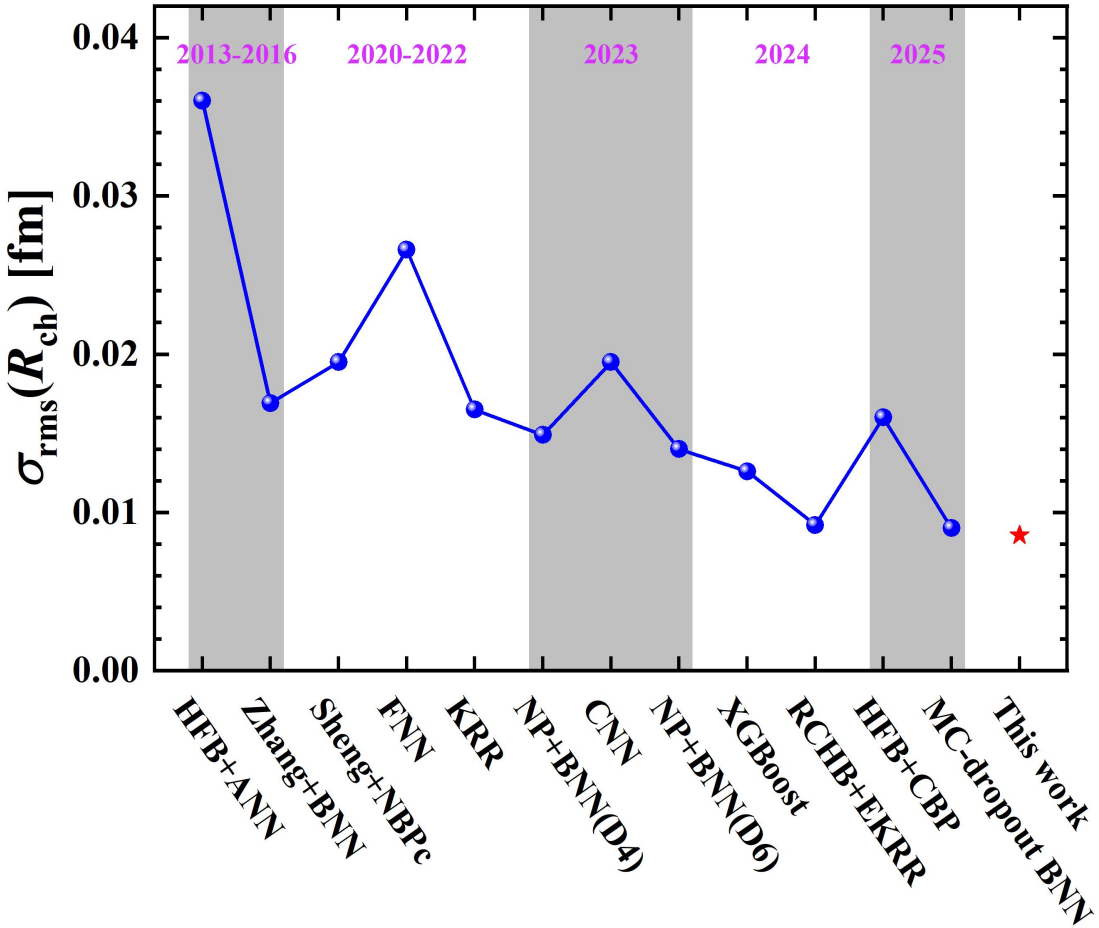


Fig. 2 Rms deviations $\sigma_{rms}(R_{ch})$ of various ML methods in Refs. [1-12] and the PIML method with respect to the experimental charge radii. The publication years are indicated at the top, and the red star denotes the result of this work.

[1] S. Akkoyun *et al.*, J. Phys. G **40**, 055106 (2013). **HFB+ANN**

[2] R. Utama *et al.*, J. Phys. G **43**, 114002 (2016). **Zhang+BNN**

[3] Y. F. Ma *et al.*, Phys. Rev. C **101**, 014304 (2020). **Sheng+NBPc**

[4] D. Wu *et al.*, Phys. Rev. C **102**, 054323 (2020). **FNN**

[5] J. Q. Ma *et al.*, Chin. Phys. C **46**, 074105 (2022). **KRR**

[6] X. X. Dong *et al.*, Phys. Rev. C **105**, 014308 (2022). **NP+BNN(D4)**

[7] Y. Y. Cao *et al.*, Nucl. Sci. Tech **34**, 152 (2023). **CNN**

[8] X. X. Dong *et al.*, Phys. Lett. B **838**, 137726 (2023). **NP+BNN(D6)**

[9] W. F. Li *et al.*, Phys. Scr. **99**, 045308 (2024). **XGBoost**

[10] L. Tang et al., Nucl. Sci. Tech. 35, 19 (2024). **RCHB+EKRR**

[11] J. Liu *et al.*, Nucl. Sci. Tech. **36**, 215 (2025). **HFB+CBP**

[12] Z. Y. Xian *et al.*, Phys. Lett. B **868**, 139662 (2025). **MC-dropout BNN**

◆ PIML approach achieves competitive predictive accuracy for nuclear charge radii.

Results and discussion

安徽大学物理学院
School of Physics Anhui University

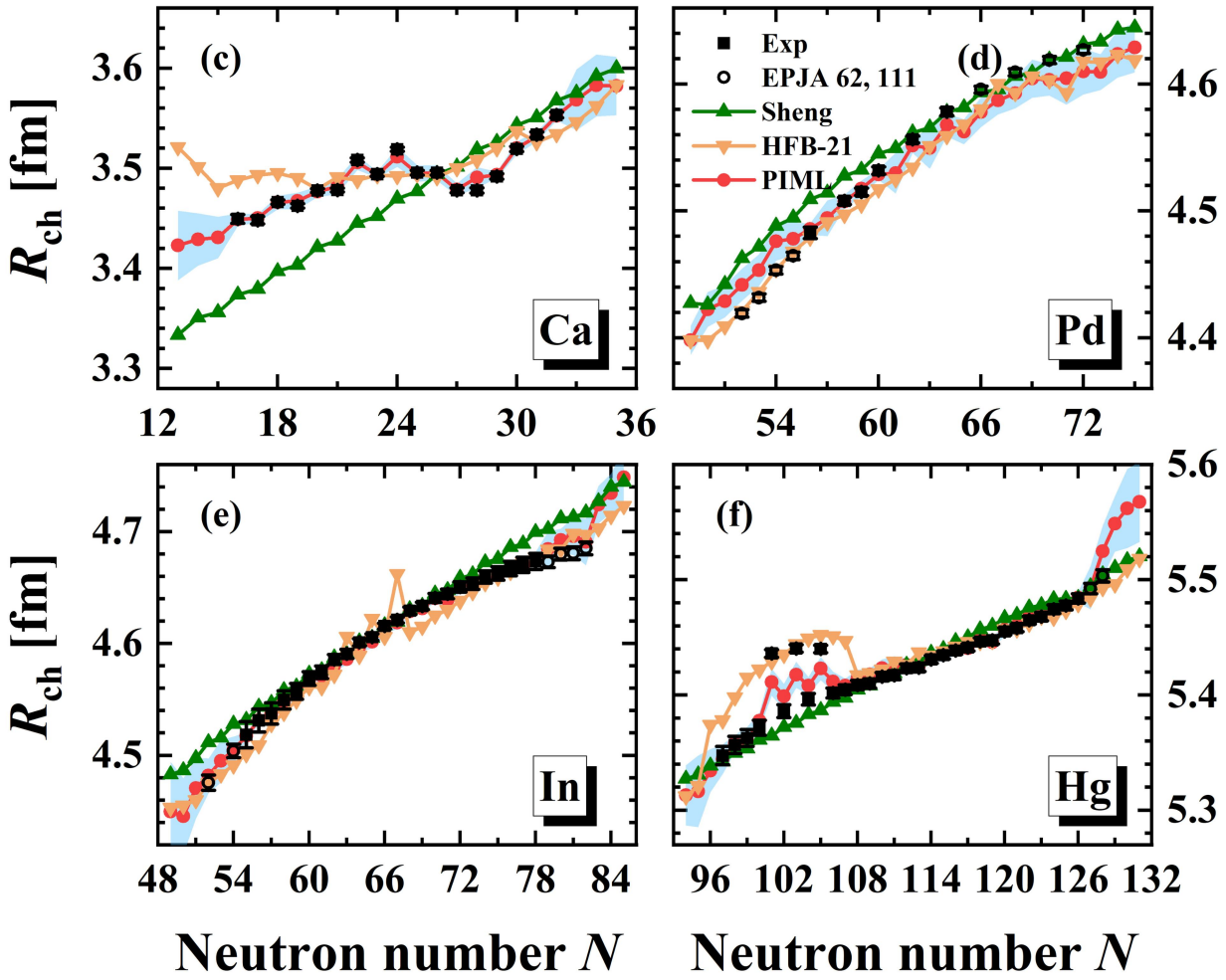
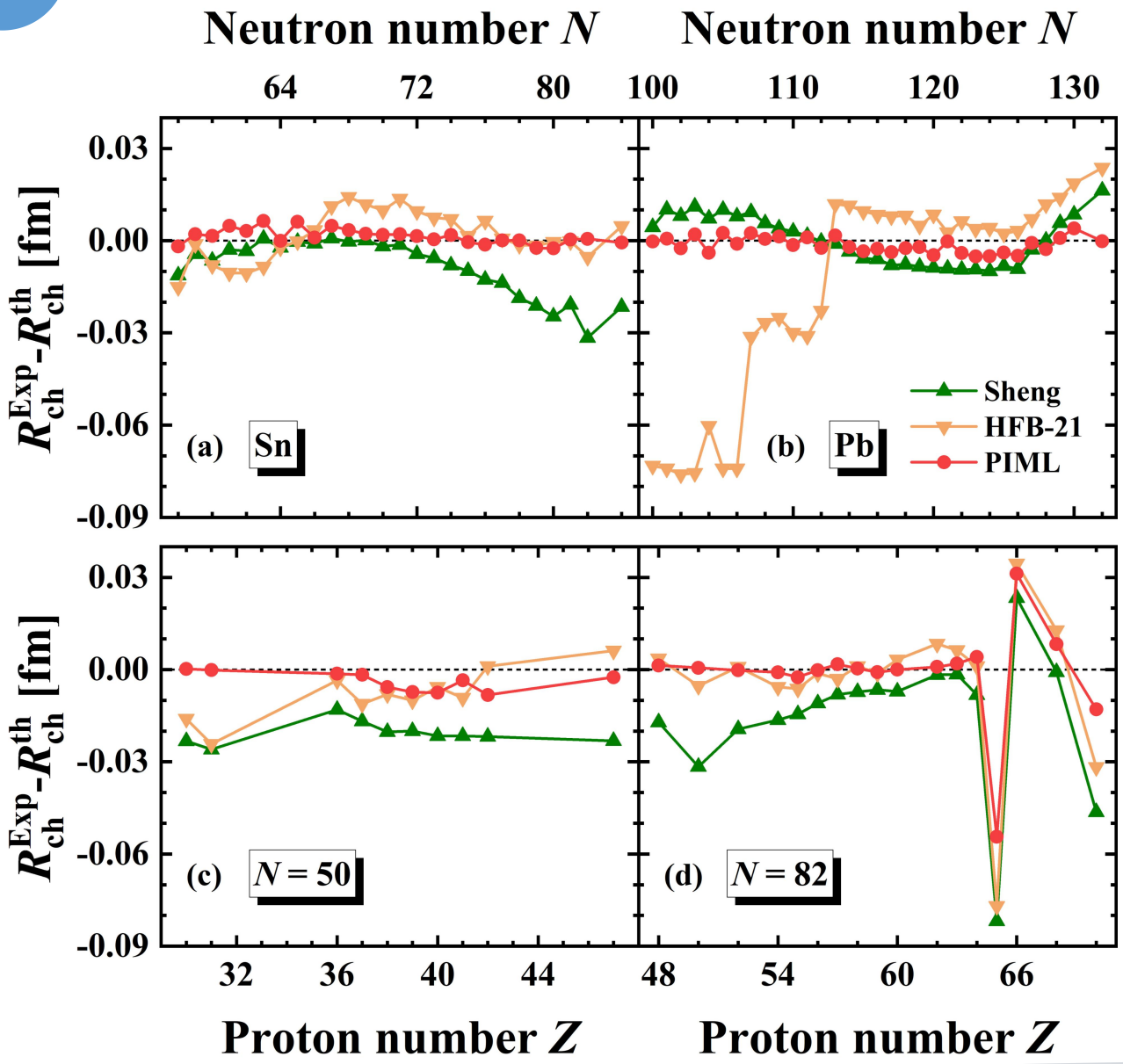


Fig. 3 Nuclear charge radii of Ca, Pd, In, and Hg isotopes. The PIML predictions and the corresponding uncertainties are shown by the filled circles and the gray-hatched regions.

- Formula Sheng gives an almost **linear increase** in charge radius with increasing neutron number.
- HFB-21 improves the description of the charge radii, while it does not reproduce the experimentally observed **odd-even staggering**.
- PIML can effectively describes all nuclear charge radii (including **Ca isotopes** and ^{181,183,185}**Hg**) within a unified framework using the same type of input.

Results and discussion



Sn and Pb isotopes:

- Formula Sheng shows larger deviations around the doubly magic region.
- HFB-21 overestimates the charge radii of neutron-deficient Pb isotopes.

***N* = 50 and 82 isotones:**

- Formula Sheng overestimates almost all experimental charge radii, a significant improvement on which is achieved by the HFB-21 and PIML.

Fig. 4 Differences between the experimental charge radii and the theoretical results obtained with Formula Sheng, HFB-21, and PIML for Sn, Pb isotopes and $N = 50$, 82 isotones.

Results and discussion

安徽大学物理学院
School of Physics Anhui University

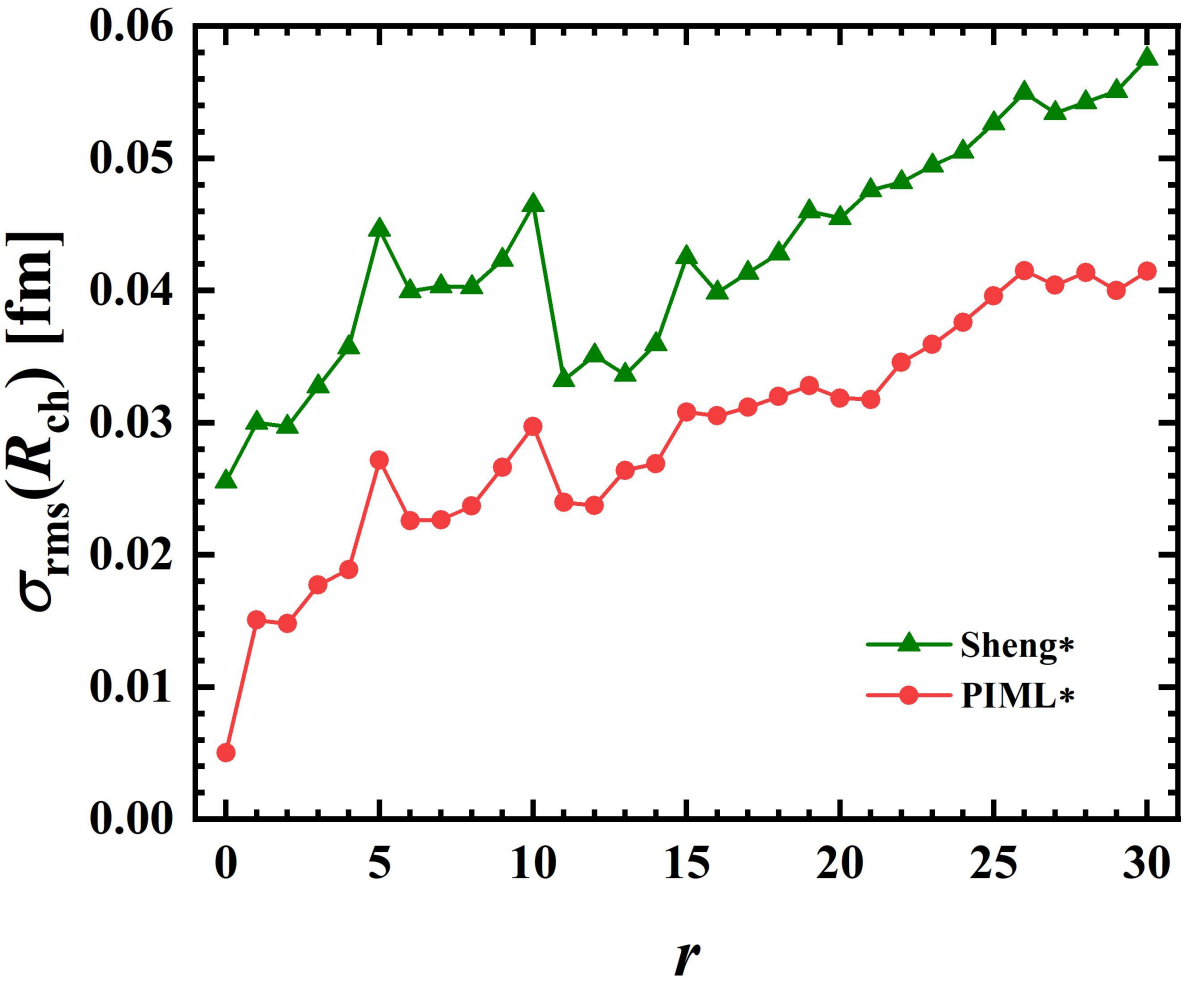


Fig. 5 Rms deviations of charge radii predicted by the Formula Sheng* and PIML* with respect to the HFB-21 predictions as a function of the minimum distance *r* to isotopes in the known region.

- Known region: Rms deviations of Formula Sheng* and PIML* are **0.0255** and **0.0050** fm, respectively.
- Unknown region: The overall trends of the two models are similar, but the rms deviations of PIML* are about **0.01 fm** smaller than those of Formula Sheng* over a wide range of extrapolation distances.
- PIML can improve both the local accuracy and the extrapolation ability by retaining the physical constraints of the empirical formula.

04 Summary and perspectives

Summary

Nuclear charge radii are studied using a physics-information machine learning approach, in which a neural network determines the nucleus-dependent parameters of a physically motivated empirical formula.

★This PIML achieves an rms deviation of **0.0086 fm** with respective to the experimental charge radii for nuclei with $Z, N \geq 8$.

★This approach can reproduce the complex charge radius evolution of **Ca and Hg isotopes** within a unified framework, and can also improve the description of charge radii for the nuclei around **magic numbers**.

★The extrapolation ability of this approach is further tested by using charge radii of HFB-21 as pseudo-experimental data.

Future perspectives

安徽大学物理学院
School of Physics Anhui University

In the future, this physics-information machine learning approach can applied to study other nuclear properties, such as nuclear masses, half-lives, and reaction cross sections.



Thank You!